EJECTION OF CLIMATE ACTIVE GASES AFTER LARGE IMPACTS. N. A. Artemieva[1,2], [1]Planetary Science Institute, Tucson AZ 85719 (artemeva@psi.edu), [2]Institute for Dynamics of Geospheres RAS, Moscow.

Introduction: Impacts are extremely hazardous on both local and global scale, and can occasionally change the course of evolution. The Chicxulub impact caused a global catastrophe and, although the principal drivers for the K-Pg mass extinction remain a matter of some debate, the ejection of dust, soot and climate-active gases (carbon dioxide, sulfur oxides, water vapor, and nitric oxide) into the atmosphere is likely to have played a significant role [1]. The main goal of the current project is to improve our understanding of large impacts and the Chicxulub impact in particular, using the most advanced hydrocode models [2] and recent improvements in the equations of state of geological materials [3].

Methods and Initial Conditions: We use the multi-phase hydrocode SOVA [4] to model impact cratering, plume formation and ejecta distribution. SOVA is a 3D Eulerian code that models multidimensional, multimaterial, large deformation, strong shock wave physics. In addition, SOVA is able to replicate the dynamics of an impact plume in comparison to other codes (e.g. CTH and iSALE) as it has the advantage of including a multi-phase hydrodynamics procedure that describes solid/molten particles in an evolving ejecta-vapor plume and their momentum-energy exchange. Recently the code was modified to include radiative transfer equations in 'dusty' environment [5] and decrease of dusty particles mass due to their ablation during re-entry [6]. The latter modification is extremely important as re-entering solid ejecta may be strongly heated [5, 7, 8]. Tracer particle technique is used to estimate maximum shock compression within target materials (hence, gas/vapor/melt production, size-frequency distribution of ejecta) and ejection velocities (hence, maximum altitude and distance to deposition).

In this paper we use a pure sedimentary target (calcite EOS) covered in some variants by water (water ANEOS). The projectile is 10 km/s in diameter, its velocity is 18 km/s, and impact angle varies from 15° to 90° to horizon.

Results are mainly presented in dimensionless form and can be easily recalculated to larger/smaller projectiles using obvious scaling parameters. The results are restricted to ejecta with velocities higher than 1 km/s. Ejecta with lower velocity cannot reach high altitudes and, hence, cannot be re-distributed globally.

Depth of excavation does not exceed one projectile radius and decreases quickly with an impact angle decrease (Fig.1). Impact angles between 45 and 60° (25% of all impacts occur in this interval) are most efficient from the viewpoint of gas production. Dependence on the sedimentary cover thickness is practically linear and similar for all impact angles except of the shallowest ones (15 and 30°).

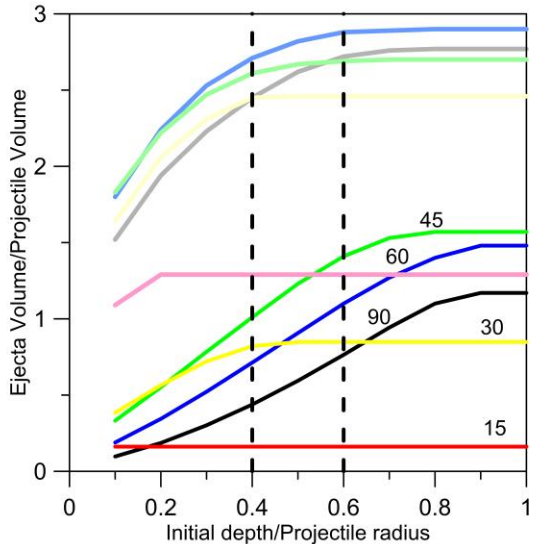

Fig. 1. Volume of ejecta excavated from a depth shallower than shown on the X-axis. Various impact angles are shown by different colors (see also numbers near the curves). Bright colors correspond to ejecta shocked above 60 GPa (potential release of CO_2 from carbonates); pale colors are for solid ejecta. Two dashed vertical lines show a possible range of the sedimentary cover thickness measured in projectile radii for the Ries and the Chicxulub craters (an exact value depends on an impact scenario). In the Haughton crater this ratio is of ~1.

Ejecta distributions over velocities are presented in Fig. 2. Highly shocked materials prevail at velocities higher than 5 km/s. At velocities lower than 3 km/s solids are the main component in ejecta for any impact angle; for velocities of 1 km/s and less the amount of gas/vapor is negligible.

Water cover. Generally, the sedimentary target is covered by water. Whereas in the Chicxulub case its thickness is small and its influence on ejection process is minimal, the average depth of the Earth's ocean is ~ 4 km, i.e., comparable with the size of 'killer' asteroids. Suite of impact models with water thickness of 0.1-1 of a projectile radius shows that the influence of water on pressure distribution is minimal whereas ejection velocities of sediments decrease dramatically (Fig.

3). Instead, water, steam, and sea salt are ejected to high altitudes.

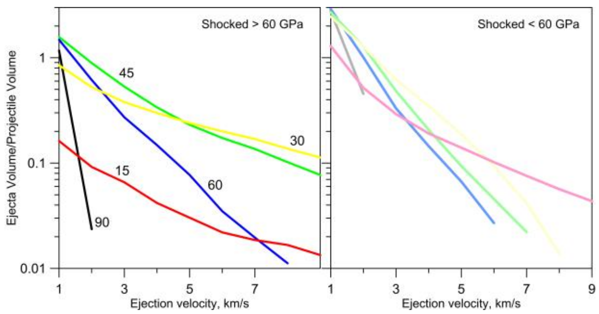

Fig. 2. Cumulative distribution of ejecta over the ejection velocity for various impact angles (see Fig.1 for the legend). Decomposed sediments are on the left, solid ejecta – on the right. At high velocities (> 5 km/s) gases prevail, whereas at low velocities their amount is negligible in comparison with solid materials.

Comparison with previous studies. Estimates of the amount of CO_2 released due to shock compression vary by an order of magnitude due to: a) uncertainties in the value of shock pressure needed for decarbonation [11, 12]; b) the rate of recombination of CO_2 with highly reactive residual oxides; c) the impact angle [10]. Moreover, due to computational cost, all previous models[10-11] were restricted to the initial few seconds after impact. Our models last at least 30s to ensure ejection from the crater. We found that at impact angles of 30-60° the amount of carbon dioxide released into the atmosphere is in the range of 2,000-2,700 Gton if the target is pure non-porous calcite. This amount is four times higher than [11] and twice smaller than the maximum estimate [10].

Discussion: The main purpose of this study is to provide GCM models with simple and reliable initial conditions related to a high-velocity impact. Some estimates are straightforward (Fig. 1-2). However, a few questions are still open.

SOx release: The production of sulfate aerosols from the release of SO_2 and water vapor into the stratosphere is well documented for volcanic eruptions. Micrometer-sized sulfate aerosols scatter visible solar radiation and can be strong absorbers of IR radiation, causing a net cooling of the Earth's surface. During the K–Pg impact, dissociation of evaporitic layers in the sediments would have produced orders of magnitude more sulfur oxides than a giant volcanic eruption. Better estimates require knowledge of evaporates content within the sedimentary cover at the Chicxulub impact site and a kinetic model for SO_2-SO_3 reactions within an impact plume.

Solid ejecta and their contribution to gas production. Solid (shocked below 60 GPa) ejecta prevail at all ejection velocities below 5 km/s. Whereas low-velocity (<1 km/s) ejecta are deposited as a continuous ejecta blanket, solid debris ejected at higher velocities may be heated about decomposition temperature of ~1100 K [8], i.e., may contribute to the net gas production. Moreover, these gases are released globally in contrast to gases produced after shock compression in a close proximity to the growing crater. However, heating of re-entering particles strongly depends not only on the total ejected mass and its velocity (which are easily calculated, see Fig. 2), but also on the size-frequency distribution of particles which depends on many factors and is currently not quite clear.

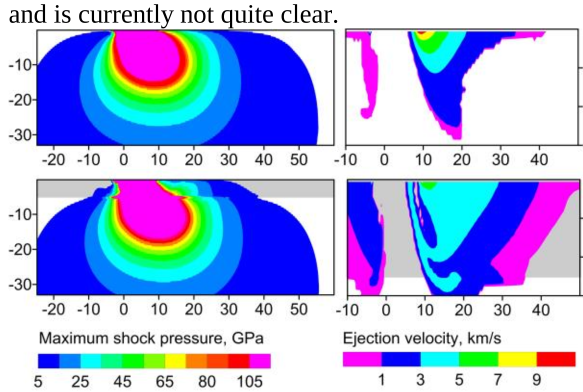

Fig. 3. Maximum shock pressure (left) and ejection velocity (right) after a 10-km-diameter asteroid impact at 60° into a sedimentary target (top) and into a similar target covered by 5-km-deep water (shown by a gray rectangular). The influence of water layer on shock compression is minimal, while ejection velocities change dramatically. Actually, there is no high-velocity CO_2 ejection after the deep oceanic impact. Distances are in km, vertical scale for the velocity map is different from the pressure map.

Acknowledgments: The study is supported by NASA grant 15-EXO15_2-0054.

References: [1] Alavarez L.W. et al. (1980 *Science, 208*, 1095-1108. [2] Pierazzo E. et al. (2008) *Meteoritics & Planet. Sci., 43*, 1917-1938. [3] Melosh H.J. (2007) *Meteoritics & Planet. Sci., 42*: 2079-2098. [4] Shuvalov V.V. (1999) *Shock Waves, 9*, 381–390. [5] Morgan J.M. et al. (2013) *JGR, 118*, 1508-1520. Author I. J. (2002) [6] Artemieva N. and Shuvalov V. (2016) *LPSC 47*, Abstract #1749. [7] Goldin T. and Melosh H.J. (2009) *Geology, 37*, 1135-1138. [8] Artemieva N. and Simonson B. (2012) *LPSC 43*, Abstract #1372. [9] Pierazzo E. (2005) *LPSC 36*, Abstract #1987. [10] Pierazzo E. and Melosh H.J. (1999) *EPSL, 165*, 163-176. [11] Pope K. et al. (1997). *JGR, 102*, 21,645–21,664. [12] Bell M.S. (2016) *Meteoritics & Planet. Sci., 51*, 619-646.